P159 from Mycoplasma hyopneumoniae Binds Porcine Cilia and Heparin and Is Cleaved in a Manner Akin to Ectodomain Shedding

ARTICLE *in* JOURNAL OF PROTEOME RESEARCH · NOVEMBER 2013

Impact Factor: 4.25 · DOI: 10.1021/pr400903s · Source: PubMed

Journal of proteome research

Article

pubs.acs.org/jpr

P159 from *Mycoplasma hyopneumoniae* Binds Porcine Cilia and Heparin and Is Cleaved in a Manner Akin to Ectodomain Shedding

Benjamin B. A. Raymond,[§,†] Jessica L. Tacchi,[§,†] Veronica M. Jarocki,[†] F. Chris Minion,[‡] Matthew P. Padula,[†] and Steven P. Djordjevic*[,†]

[†]The ithree institute, University of Technology Sydney, PO Box 123, Broadway, NSW 2007, Australia

[‡]Department of Preventive and Veterinary Medicine, Iowa State University, 2180 Veterinary Medicine, Ames, Iowa 50011, United States

Supporting Information

ABSTRACT: *Mycoplasma hyopneumoniae* colonizes the ciliated epithelial lining of the upper respiratory tract of swine and results in chronic infection. Previously, we have observed that members of P97 and P102 paralog families of cilium adhesins undergo endoproteolytic processing on the surface of *M. hyopneumoniae*. We show that P159 (MHJ_0494), an epithelial cell adhesin unrelated to P97 and P102 paralog families, is a cilium adhesin that undergoes dominant cleavage events at S/T-X-F↓X-D/E-like motifs located at positions ^{233}F↓Q^{234} and ^{981}F↓Q^{982}, generating P27, P110, and P52. An unrelated cleavage site ^{738}L-K-V↓G-A-A^{743} in P110 shows sequence identity with a cleavage site (L-N-V↓A-V-S) identified in the P97 paralog, Mhp385, and generates 76 (P76) and 35 kDa (P35) fragments. LC−MS/MS analysis of biotinylated surface proteins identified six peptides with a biotin moiety on their N-terminus indicating novel, low abundance neo-N-termini. LC−MS/MS of proteins separated by 2D-PAGE, 2D immunoblotting using monospecific antiserum raised against recombinant fragments spanning P159 ($F1_{P159}$-$F4_{P159}$), and proteins that bound to heparin-agarose were all used to map P159 cleavage fragments. P159 is the first cilium adhesin not belonging to the P97/P102 paralog families and is extensively processed in a manner akin to ectodomain shedding in eukaryotes.

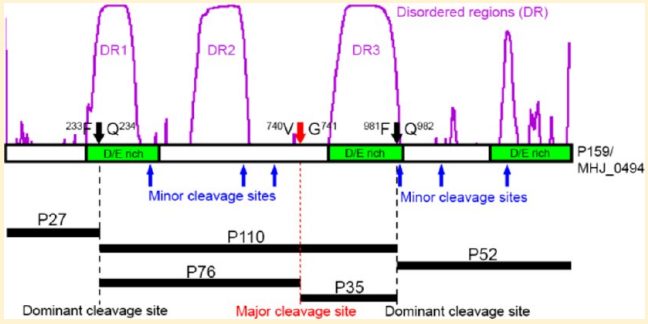

KEYWORDS: *endoproteolytic cleavage, protein processing, glycosaminoglycan-binding protein, heparin, functional redundancy, protein disorder, coiled coils, ectodomain shedding*

INTRODUCTION

Mycoplasma hyopneumoniae remains an economically significant threat to the health of swine despite widespread vaccination with bacterin formulations. Vaccination reduces lung pathology and improves weight gain but fails to prevent colonization of the respiratory tract by *M. hyopneumoniae*.[1−5] *M. hyopneumoniae* is a genome-reduced, swine-specific bacterial pathogen, and the number of predicted open reading frames (ORFs) determined by in silico analysis of the genome sequences of four geographically diverse strains (232, J, 7448, 168) is ∼700.[6]

M. hyopneumoniae preferentially colonizes the surface of cilia and microvilli on porcine respiratory epithelium.[7,8] Cilium and epithelial cell adhesion is a complex process involving a number of cell surface proteins, many of which belong to the P97 and P102 paralog adhesin families. The P97 and P102 adhesin families each share 30% sequence identity[6] and display redundant functions as cilium, fibronectin, plasminogen, and glycosaminoglycan-binding proteins. Genes encoding six paralogs of the archetype cilium adhesin P97 (MHJ_0369/Mhp385, MHJ_0264/Mhp107, MHJ_0663/Mhp684, MHJ_0096/Mhp280, MHJ_0105/Mhp271, MHJ_0493/Mhp493) and six paralogs of P102 (MHJ_0368/Mhp384, MHJ_0263/Mhp108, MHJ_0662/Mhp683, MHJ_0104/Mhp272, Mhp274, and Mhp275) from strains J and 232, respectively, are conserved.

Whereas P97 and P102 and their paralogs are heavily expressed during broth culture, they are presented on the membrane surface of *M. hyopneumoniae* as cleavage fragments derived by endoproteolytic processing.[9−16] Dominant processing events are typically confined to the carboxyl side of phenylalanine residues within the motif S/T-X-F↓X-D/E.[9] Other cleavage motifs are believed to play a role in shaping the surface protein topography of *M. hyopneumoniae*, but some of these have not been experimentally verified.[10−12] Members of the P97 and P102 families often carry coiled-coil motifs and expansive regions of protein disorder spanning more than 40 consecutive amino acids.[9−11,17] Dominant cleavage sites that adhere to the S/T-X-F↓X-D/E motif typically reside within disordered regions,[9−11,17] suggesting that disorder can influence

Received: September 2, 2013
Published: November 6, 2013

the accessibility of cleavage motifs in the preprotein to proteolytic cleavage. The most abundant cleavage fragments derived from P97 and P102 paralog families are multifunctional cilium adhesins that bind glycosaminoglycans,[9−11,14,16−19] fibronectin,[10,13−15] and plasminogen.[13−15,17] The ability to bind highly sulphated glycosaminoglycans is considered to be significant during the early stages of colonization because heparin effectively blocks binding of *M. hyopneumoniae* to porcine respiratory tract cilia.[10,18,20] Surface proteins of *M. hyopneumoniae* that do not belong to the P97 and P102 paralog families also bind glycosaminoglycans and plasminogen, underscoring the importance of these interactions to the survival of the species.[21]

P159 (Mhp494) is not a member of the P97 and P102 paralog families, yet it is known to be a cellular adhesin.[18] The P159 homologue from strain 232 comprises 1410 amino acids and is processed to form N-terminal, central, and C-terminal fragments of 27 (P27), 110 (P110), and 52 kDa (P52) respectively, and these cleavage fragments are presented on the surface of *M. hyopneumoniae*. Previously, we examined the functions of these three dominant cleavage products by expressing four polyhistidine-tagged proteins ($F1_{P159}$-$F4_{P159}$ spanning amino acids 31−264, 265−519, 558−909, and 958−1405, respectively) in *Escherichia coli*. P159 is not detectable by SDS-PAGE or by immunoblotting using serum against F2−$F4_{P159}$. C-terminal recombinant fragments $F3_{P159}$ and $F4_{P159}$ bound heparin, and latex beads coated with recombinant fragments $F2_{P159}$−$F4_{P159}$ displayed the ability to adhere to porcine kidney epithelial-like (PK-15) cells.[18] P159 is subject to further cleavage events because Western blots exposed to antiserum raised against $F2_{P159}$ and $F3_{P159}$ identified 76 (P76) and 35 kDa (P35) cleavage fragments and numerous less abundant fragments.[18] We were unable to determine the precise cleavage sites that generate P27, P52, or P110 in our previous study but showed that cleavage events were confined to regions spanning amino acids 219−303 and 841−978.[18]

Our proteome data indicate that P159 is abundantly expressed. Here we have characterized the precise endoproteolytic cleavage events that define the dominant (P27, P110, P52) and major (P76, P35) cleavage fragments and assessed the ability of recombinant fragments $F1_{P159}$−$F4_{P159}$ spanning P159 to bind to porcine respiratory tract cilia. We also provide compelling evidence that P159 is extensively processed, generating numerous surface-accessible cleavage fragments, many of which retain the ability to bind glycosaminoglycans. Processing requires the activity of different proteases and generates a large combinatorial library of cleavage fragments that create functional diversity on the surface of *M. hyopneumoniae*.

MATERIALS AND METHODS

Culture Conditions

M. hyopneumoniae (strain J) was grown in modified Friis broth[22] and harvested, as previously described.[23]

Cell-Surface Analyses

Cell-surface biotinylation was carried out as previously described[9] on intact cells using EZ-link sulfo-NHS-biotin [Thermo Fischer Scientific], combined with avidin column purification or blotting to purify or identify biotinylated surface proteins.[9,24] Enzymatic cell surface shaving with trypsin was also used as previously described.[10] Liberated surface proteins were collected, reduced and alkylated, and further digested to peptides with trypsin for LC−MS/MS analysis, as previously described.[25]

Preparation of *M. hyopneumoniae* Whole Cell Lysate

Procedures used to generate whole cell lysates of *M. hyopneumoniae* have been previously described.[15] In brief, a 0.1 g pellet of *M. hyopneumoniae* cells was resuspended in solubilization buffer (7 M urea, 2 M thiourea, 40 mM Tris, 1% (w/v) C7BzO) and disrupted with four rounds of sonication at 50% power for 30 s bursts on ice. Proteins were reduced and alkylated with 20 mM acrylamide monomers and 5 mM tributylphosphine for 90 min. Insoluble material was pelleted by centrifugation. Protein was precipitated in five volumes of ice-cold acetone for 30 min, and the pellet was air-dried. Protein pellet was resolubilized in 7 M urea, 2 M thiourea, and 1% (w/v) C7BzO supplemented with 0.2% 3−10 BioLyte ampholytes [BioRad] for 2D separation.

One- and Two-Dimensional Gel Electrophoresis and Immunoblotting

A detailed protocol for performing 1D and 2D gel electrophoresis and immunoblotting has been described previously.[11] For 1D gel electrophoresis, proteins were separated by SDS-PAGE, and gels were fixed and visualized by staining with either Flamingo fluorescent gel stain [BioRad] or Coomassie Blue G-250. For 2D gel analyses, 250 μg of protein was cup-loaded onto partially rehydrated 11 cm pH 4−7 IPG strips [BioRad] or 6−11 Immobiline drystrips [GE Healthcare]. Focusing was performed in a BioRad Protean IEF cell at a constant 20 °C and 50 μA current limit per strip with a three-step program: slow ramp to 4000 V for 4 h, linear ramp to 10 000 V for 4 h, then 10 000 V until 120 kVh was reached. Following IEF, the strips were equilibrated with 5 mL of equilibration solution (2% SDS, 6 M urea, 250 mM Tris-HCl pH 8.5, 0.0025% (w/v) bromophenol blue) for 20 min before the second-dimension SDS-PAGE. *M. hyopneumoniae* proteins separated by 1D or 2D SDS-PAGE were blotted onto PDVF membrane using a semidry transfer method.[26] Membranes were blocked with 5% (w/v) skim milk powder in PBS with 0.1% Tween 20 (v/v) (PBS-T) at room temperature for 1 h and incubated with $F1_{P159}$−$F4_{P159}$ polyclonal antisera (diluted 1:100 in PBS-T) for 1 h at room temperature. Blots were washed and exposed to peroxidase conjugated anti-rabbit antibodies (diluted 1:3000 in PBS-T) for 1 h. Membranes were routinely washed in three changes of PBS-T and developed with SIGMA*FAST* 3,3′-diaminobenzidine tablets [Sigma-Aldrich] as per manufacturer's instructions.

Affinity Chromatography

M. hyopneumoniae whole cell lysates were prepared by sonicating washed cell pellets in 10 mM sodium phosphate, pH 7 on ice for three rounds of 30 s bursts. Insoluble material was pelleted by centrifugation at 16 000*g* for 10 min. *M. hyopneumoniae* soluble protein (300 μg) was loaded into an autosampler vial on a Waters 2690 Alliance LC separations module and loaded at 0.5 mL min^{-1} onto a 1 mL HiTrap Heparin HP column [GE healthcare] in binding buffer (10 mM sodium phosphate, pH 7). The standard elution program was run at 0.5 mL min^{-1} with continuous gradients as follows: Sample was loaded and washed with 100% binding buffer (20 min) followed by 0−50% elution buffer (10 mM sodium phosphate, 2 M sodium chloride, pH 7) (25 min), 50−100% elution buffer (10 min), and 100% elution buffer (5 min) before returning to 100% binding buffer. The elution profile

dx.doi.org/10.1021/pr400903s | J. Proteome Res. 2013, 12, 5891−5903

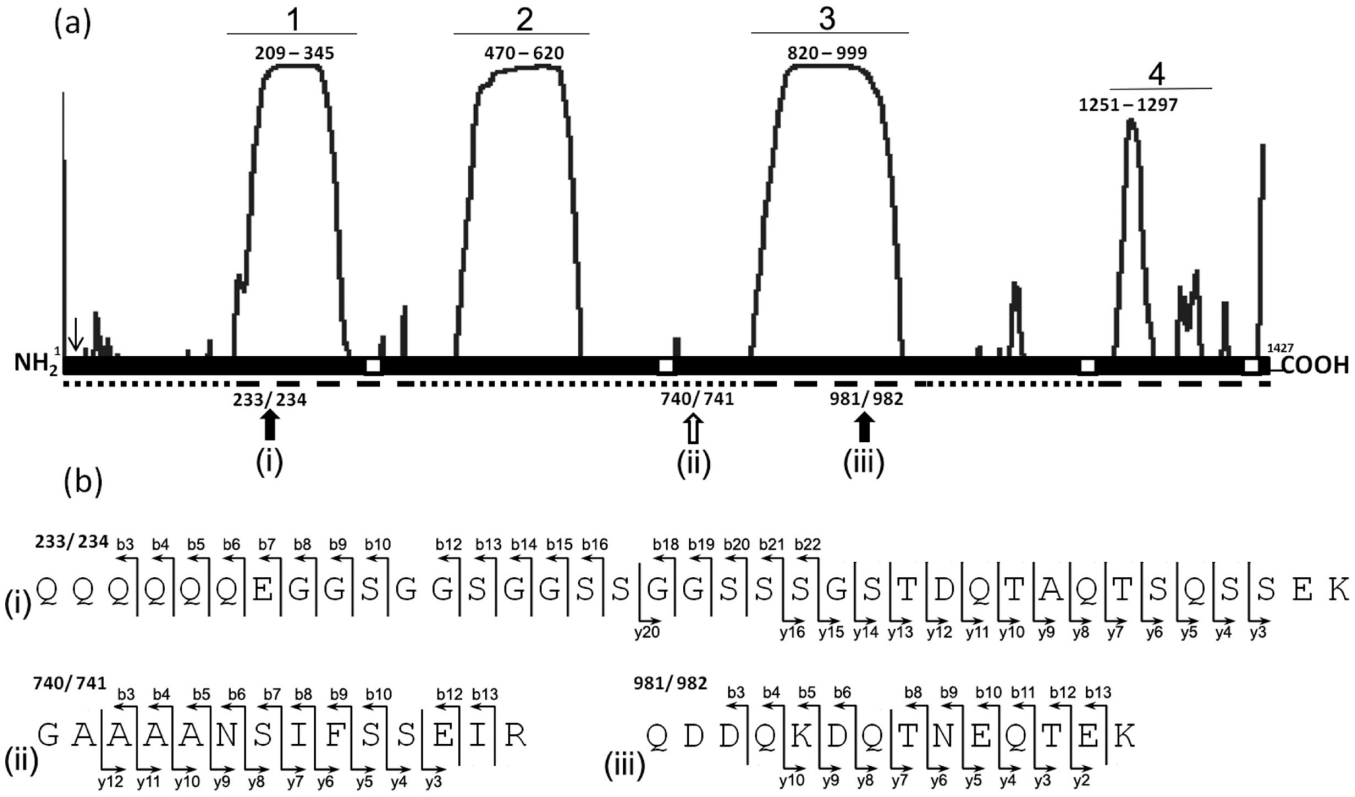

Figure 1. Structural analysis of P159. (a) Regions of disorder within P159 (black bar) as peaks above the molecule, labeled 1, 2, 3, and 4, predicted by PONDR VSL1.[30] Dominant cleavage sites are shown by solid black arrows (i,iii), and a major cleavage site is represented by a hollow arrow (ii). Coiled-coil regions as predicted by COILS[29] are shown by white boxes. Small dashed lines represent regions within P159 that are rich in basic amino acids, and larger dashed lines represent those rich in acidic amino acids. (b) Sequences of semitryptic peptides identified at positions i–iii, as indicated in panel a, denoting the N-terminus of cleavage fragments. Spectra are shown in Supplementary Figure S1 in the Supporting Information.

was monitored at A = 210–400 nm with a Waters 996 photodiode array detector, and fractions were collected in 3 min intervals using a Waters fraction collector III.

1D LC–MS/MS Using QTOF

Sample (10 μL) was loaded at 20 μL min^{-1} with MS buffer A (2% acetonitrile +0.2% formic Acid) onto a C8 Cap Trap column [Michrom, USA] using an Eksigent AS-1 autosampler connected to a Tempo nanoLC system [Eksigent, USA]. After the trap was washed for 180 s, the peptides were washed off the trap (300 nL min^{-1}) onto an IntegraFrit column (75 μm × 100 mm) packed with ProteoPep II C18 resin [New Objective, Woburn, MA]. Peptides were eluted from the column and into the source of a QSTAR elite hybrid quadrupole-time-of-flight mass spectrometer [Applied Biosystems/MDS Sciex] using the following program: 5–50% MS buffer B (98% acetonitrile +0.2% formic acid) over 30 min for gel slices or 15 min for gel spots, 50–80% MS buffer B over 5 min, and 80% MS buffer B for 2 min, 80–5% for 3 min. The eluting peptides were ionized with a 75 μm ID emitter tip that tapered to 15 μm [New Objective] at 2300 V. An Intelligent Data Acquisition (IDA) experiment was performed, with a mass range of 375–1500 Da continuously scanned for peptides of charge state 2+ to 5+ with an intensity of more than 30 counts/scan and a resolution >12 000. Selected peptides were fragmented, and the product ion fragment masses were measured over a mass range of 100–1500 Da. The mass of the precursor peptide was then excluded for 120 s for gel slices or 15 s for gel spots.

MS/MS Data Analysis

The MS/MS data files were searched using Mascot (provided by the Australian Proteomics Computational Facility, hosted by the Walter and Eliza Hall Institute for Medical Research Systems Biology Mascot Server) against the LudwigNR database (composed of the UniProt, plasmoDB and Ensembl databases (vQ312. 19 375 804 sequences; 6 797 271 065 residues)) with the following parameter settings. Fixed modifications: none. Variable modifications: propionamide, oxidized methionine. Enzyme: semitrypsin. Number of allowed missed cleavages: 3. Peptide mass tolerance: 100 ppm. MS/MS mass tolerance: 0.2 Da. Charge state: 2+ and 3+. For biotinylated samples, variable modifications also included biotinylated lysine and N-terminal biotinylation.

Avidin Purification of Interacting Proteins

To identify *M. hyopneumoniae* proteins that bind to surface proteins on porcine kidney (PK15) epithelial cells, we used a protocol adapted from Chen et al.[27] One 175 cm^2 culture flask containing semiconfluent PK-15 cells was washed three times with ice-cold PBS (pH 8.0) to remove medium components. Cells were detached by incubating with TrypLE Express [Life Technologies] for 10 min at room temperature. Cells were washed twice with PBS by centrifugation to remove any excess reagent. Cells were then labeled with 2 mM EZ-link sulfo-NHS-biotin (4 °C for 30 min) with gentle inversion. PBS with 100 mM glycine was added to quench the reaction and remove excess biotin (10 min at room temperature). Glycine was removed by washing twice in PBS. Cells were lysed in 1.0%

dx.doi.org/10.1021/pr400903s | J. Proteome Res. 2013, 12, 5891–5903

Triton X-100 in Tris-HCl pH 7.6, 150 mM NaCl with protease inhibitors on ice (30 min) with vortexing. After insoluble material was removed by centrifugation, the cleared lysate was added to avidin agarose [Thermo Scientific] and incubated (1 h at room temperature) on a rotating wheel. The slurry was then packed into a column, and the flow through was collected for monitoring by SDS-PAGE. Unbound proteins were removed by six washes with PBS.

M. hyopneumoniae cells from a 250 mL culture were pelleted, washed with PBS, and gently lysed in 0.5% Triton X-100 in Tris-HCl pH 7.6, 150 mM NaCl with protease inhibitors on ice with vortexing and water bath sonication. Insoluble material was removed by centrifugation at 16 000*g* for 10 min, and the cleared lysate was incubated with the biotinylated PK-15-avidin agarose mixture overnight at 4 °C on a rotating wheel. The mixture was packed into a column, the flow through was collected, and noninteracting proteins were removed by washing six times with 25 mM Tris-HCl in 150 mM NaCl, pH 7.4. Interacting proteins were collected by eluting five times with 100 mM Tris-HCl in 2 M NaCl, pH 7.4. A secondary elution in 30% acetonitrile and 0.4% trifluoroacetic acid was performed to collect the biotinylated PK-15 proteins and any strongly bound *M. hyopneumoniae* proteins that were not eluted by 2 M NaCl. The salt and acidic elutions were concentrated separately through 3000 Da cutoff filters, then acetone precipitated at −20 °C for 30 min, and finally pelleted by centrifugation at 25 000*g* at 4 °C for 30 min. Protein was resuspended in SDS sample buffer and separated by 1D SDS-PAGE. Proteins were in-gel trypsin digested and analyzed by LC−MS/MS.

Bioinformatic Analyses of P159

Bioinformatic analysis of P159 used online resources: ProtParam,[28] COILS,[29] and PONDR VSL1.[30]

RESULTS

P159 Is an Endoproteolytically Processed, Modular Cell Surface Protein

The J strain homologue of P159 MHJ_0494 [Swiss-Prot: Q4A9J1] comprises 1427 amino acids and has a predicted p*I* of 8.05. P159 carries almost identical numbers of positively charged (198 K/R residues) and negatively charged (195 D/E residues) amino acids, but their arrangement in the sequence is unevenly distributed. Analysis of charge distribution shows that P159 is a modular protein that contains three acidic domains, ∼200 amino acids in length, that are enriched in aspartic acid (D) and glutamic acid (E) residues spanning amino acids 200−370 (acidic domain 1; p*I* 5.7), 820−1000 (acidic domain 2; p*I* 4.8), and 1230−1427 (acidic domain 3; p*I* 5.8). Four regions spanning a minimum of 40 amino acids that display protein disorder were identified in P159 using PONDR and PrDOS algorithms, and four coiled-coil regions were identified using EMBnet COILS (Figure 1). Of four regions displaying protein disorder, domains 1, 3, and 4 align closely with acidic domains (Figure 1).

Identification of Cleavage Sites That Generate P27, P110, and P52

Recently, we reported the location of dominant endoproteolytic cleavage sites bearing an S/T-X-F↓X-D/E motif within regions of protein disorder in members of the P97 and P102 paralog families.[9,11,17] P159 is not a member of the P97 and P102 paralog families, but it is a target of endoproteolytic processing so much so that P159 is undetectable by SDS-PAGE. These cleavage events generate N-terminal 27 kDa (P27), central 110 kDa (P110), and C-terminal 52 kDa (P52) fragments, representing the major effector molecules of P159.[18] While we were previously unable to define the precise cleavage sites that created these fragments, cleavage sites were localized to regions spanning amino acids 219−303 and 841−978 in the P159 homologue in *M. hyopneumoniae* strain 232,[18] which shares 95.6% sequence identity at the amino acid level with the strain J homologue. LC−MS/MS analysis of whole cell lysates described in Seymour[15] identified a large semitryptic peptide spanning 37 amino acids (position 234−270), which defined the cleavage site that generated P27 to reside within the sequence ^{231}T-E-F↓Q-Q-Q-Q-Q-Q^{239} with cleavage occurring at position 233 after the phenylalanine reside (Figure 1b). Dominant cleavage sites in P97 and P102 paralog family members have been known to follow a phenylalanine (F) residue that precedes a short run of glutamine residues (Q).[9,11] The same approach was used to identify the cleavage site that generates P52 in the sequence ^{979}T-T-F↓Q-D-D^{984} with cleavage occurring at the phenylalanine residues at position 981. Spectra that confirm the identities of these cleavage site peptides are shown in Figure S1 in the Supporting Information.

Identification of Cleavage Fragments of P159 by 2D SDS-PAGE and LC−MS/MS

We previously constructed four recombinant polyhistidine fusion proteins ($F1_{P159}$−$F4_{P159}$) spanning regions along P159 and generated polyclonal antisera against each of these proteins.[18] To identify processing events in P159, we performed LC−MS/MS analysis on all *M. hyopneumoniae* strain J protein spots separated by 2D SDS-PAGE using immobilized pH gradients from 4−7 and 6−11 (Figure 2). The

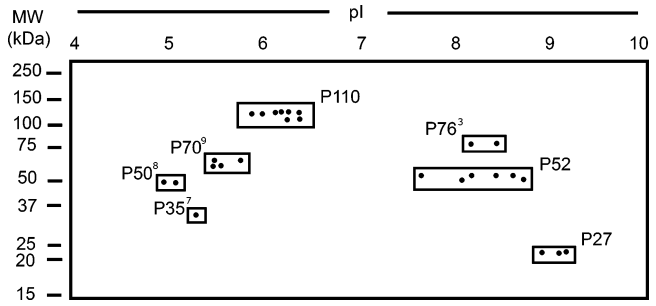

Figure 2. Mock 2D gel indicating locations of spots containing peptides mapping to P159. Seven distinct fragments of P159 were identified from 2D gels. Superscript numbers correspond to fragments described in Figure 8.

identities of P27, P110, and P52 in strain J were confirmed by LC−MS/MS of tryptic peptides generated from protein spots shown in Figure 2. In addition, four cleavage fragments within the central 110 kDa fragment of P159 (P110) were identified, two of which represent N-terminal 76 kDa (P76) and C-terminal 35 kDa (P35) fragments (Figure 2). P35 (Fragment 7) comprises 240 amino acids (position 741−981), spans most of acidic domain 2, and migrates with a p*I* of 5.25. P35 was identified in a short spot train with a mass of 35 kDa and p*I* of 5.3 in 2D immunoblots probed only with anti-$F3_{P159}$ serum (Figure 3). Loss of P35 from the C-terminus of P110 generates P76, which comprises amino acids 234−740 and migrates with a p*I* of 8.48 (Figure 2). This is consistent with a ∼75 kDa spot train (Fragment 3) on 2D immunoblots probed separately with

dx.doi.org/10.1021/pr400903s | J. Proteome Res. 2013, 12, 5891−5903

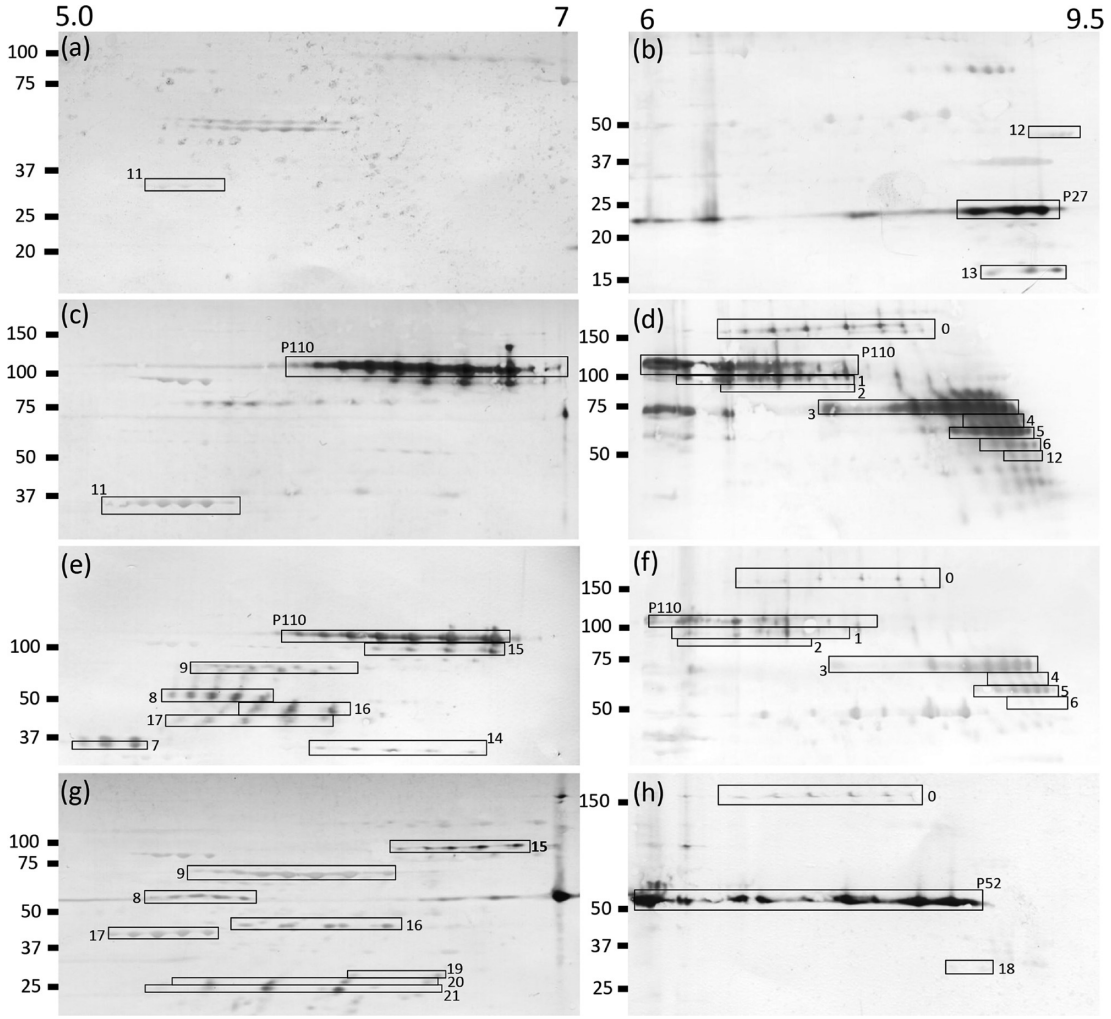

Figure 3. 2D Immunoblots probed with $F1_{P159}$–$F4_{P159}$. The left column of gels represents proteins that were separated in the pH 4–7 range, and the right column are those that were separated in the pH 6–11 range. Blots were probed with anti-$F1_{P159}$ (a,b), anti-$F2_{P195}$ (c,d), anti-$F3_{P159}$ (e,f), and anti-$F4_{P159}$ (g,h). Cleavage fragments reported by Burnett et al.[18] are labeled, and novel cleavage fragments are boxed and numbered.

anti-$F2_{P159}$ and anti-$F3_{P159}$ (Figure 3). Both P35 and P76 migrate abnormally during SDS-PAGE because their predicted masses are 28 and 56 kDa, respectively. We attribute the abnormal migration during SDS-PAGE to the pockets of acidic residues found in the N-terminus of P76 and most of P35. Consistent with these data, a semitryptic cleavage peptide ^{741}GAAAANSIFSSEIR^{754} (Figure 1b), which delineates the N-terminus of P35, was identified by LC–MS/MS. We also identified the sequence GAAAANSIFSS by Edman degradation of a protein eluted from a protein spot containing P35 (data not shown).

Two novel cleavage fragments with p*I* between 4.9 and 6.0 with masses of 50 (P50; Fragment 8) and 70 kDa (P70; Fragment 9), respectively, were also observed. These cleavage fragments span regions within P159 lacking K and R residues, and tryptic peptides generated from protein spots representative of these two cleavage fragments do not provide comprehensive coverage to accurately map their identities. Nonetheless, P50 has its N-terminus at the same position as P35, as we also identified the N-terminal semitryptic peptide ^{741}GAAAANSIFSSEIR^{754} by LC–MS/MS of P50-containing spots (Figure S1 in the Supporting Information). Thus, the P50 sequence must extend past the ^{979}T-T-F↓Q-D-D^{984} cleavage site into the N-terminus of P52 but by how many amino acids cannot be determined at this time. P50 is present as a ~50 kDa spot train on 2D immunoblots (Fragment 8; Figure 3) probed separately with anti-$F3_{P159}$ and anti-$F4_{P159}$ serum. LC–MS/MS analysis of spots containing P70 generated almost identical tryptic peptide coverage as P35 except that we identified the tryptic peptide ^{740}VGAAAASNIFSSEIR^{754} (Figure S1 in the Supporting Information). These data suggest that P70 encompasses all of P35 but contains sequences that overlap with P76 at its N-terminus and P52 at its C-terminus. Proteins of 35 (P35), 50 (Fragment 8), and 70 kDa (Fragment 9) were all detected by anti-$F3_{P159}$ serum on 2D immunoblots with p*I* from 5.3 to 6.2. Unlike P35, Fragments 8 (P50) and 9 (P70) also reacted with anti-$F4_{P159}$ on 2D immunoblots (Figure 3), indicating that they both contain sequences within P52.

The majority of fragments were identified to occur in spot trains, comprising proteoforms of varying isoelectric point. Previous studies have indicated that post-translational modifications such as phosphorylation occur in *M. hyopneumoniae* and other Mycoplasma species in proteins that resolve as spot trains during 2D SDS-PAGE.[16,31] Spot trains could be due to various modifications reflecting bona fide post-translational modifications that alter the isoelectric point or are an artifact generated during sample preparation.[32]

dx.doi.org/10.1021/pr400903s | *J. Proteome Res.* 2013, 12, 5891–5903

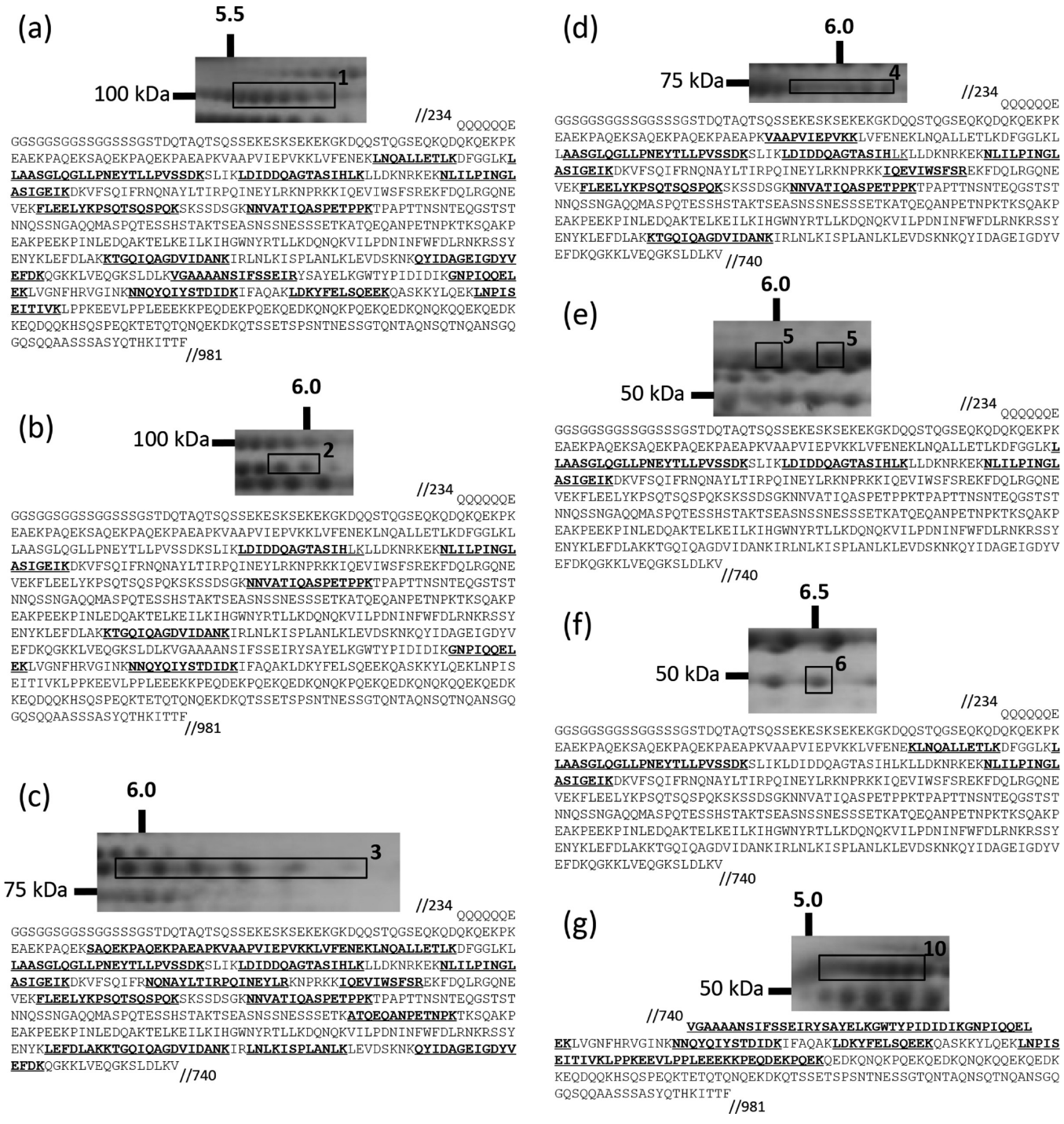

Figure 4. Biotinylated *M. hyopneumoniae* surface proteins captured by avidin chromatography resolved by 2D PAGE. Peptides spanning P159 are underlined in each panel and were identified by LC−MS/MS from single spots or a train of spots in the corresponding gel image. Spot numbers correspond to Figure 8.

Identification of Lower Abundance Cleavage Fragments of P159

We employed several approaches to identify low abundance cleavage fragments. *M. hyopneumoniae* cells were briefly exposed to sulfo-NHS-biotin. Biotinylated proteins were recovered by affinity chromatography and characterized by LC−MS/MS. Tryptic fragments that carry a biotin adduct on the N-terminal amine group represent bona fide neo N-termini. 2D immunoblots of whole cell protein preparations using p*I* gradients from 4−7 and 6−11 were probed with F1−F4$_{P159}$ antisera to determine if cleavage was consistent with the location of these N-termini. We identified ∼60 unique spots on 2D blots indicating that P159 is a target of multiple processing events (Figure 3). Enrichment protocols where LC−MS/MS was used to characterize P159 fragments recovered from heparin agarose proved useful to identify peptides mapping to low abundance cleavage fragments.

Blots probed with anti-F1$_{P159}$ reacted strongly with P27, as expected, and identified a 17 kDa fragment (Fragment 13) with a p*I* of ∼9 (Figure 3b). LC−MS/MS analysis of *M.*

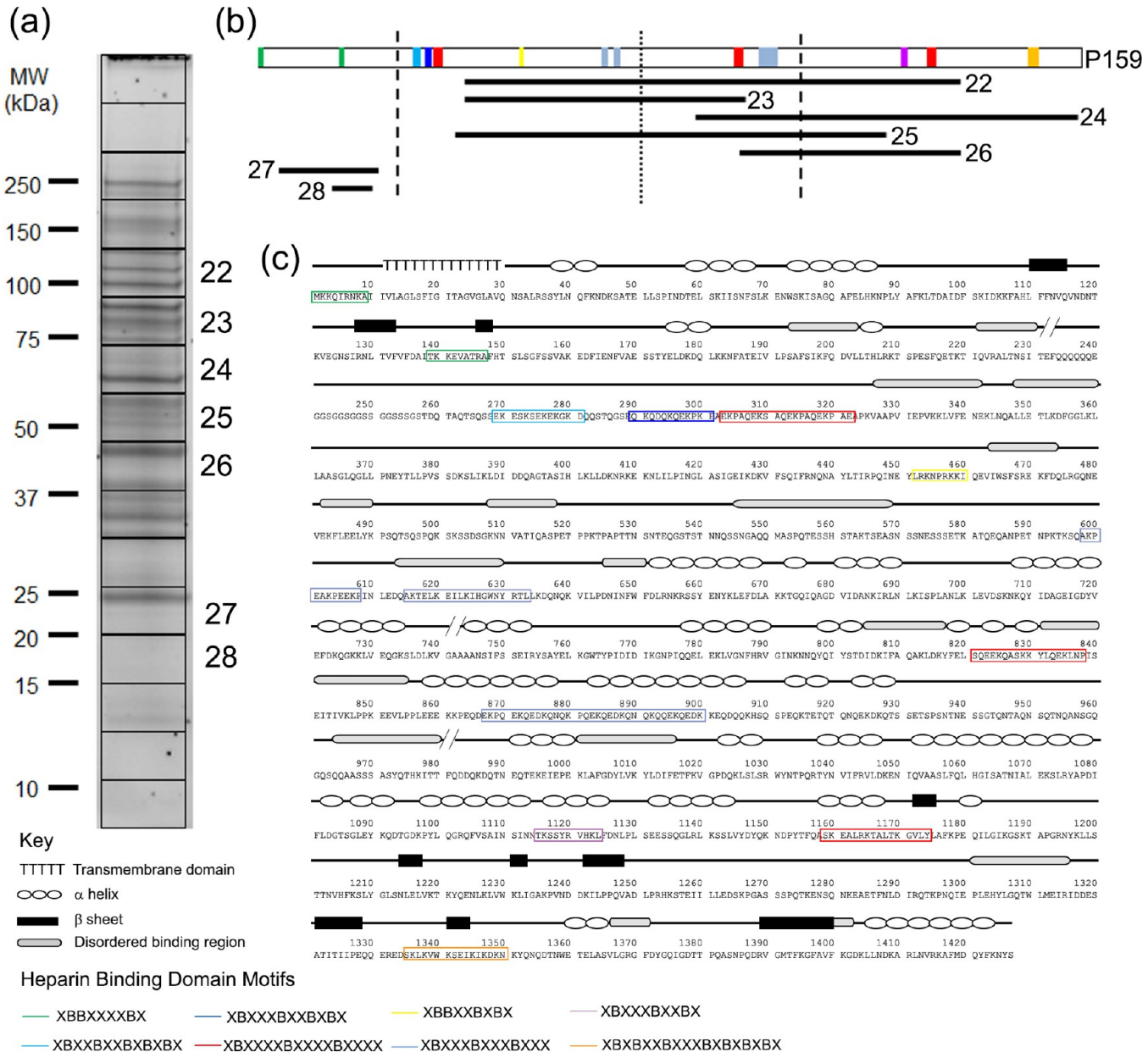

Figure 5. Schematic representation of P159 heparin-binding domain motifs and heparin-binding fragments. (a) 1D gel of *Mycoplasma hyopneumoniae* heparin-binding proteins with slices containing peptides matching to P159 fragments. (See also Figure 8.) (b) Locations of heparin-binding motifs in the box (color-coded to positions indicated in panel c) and identified fragments of P159 from the most N-terminal to the most C-terminal peptide matched. Fragments may extend beyond these boundaries. Heavy dashed vertical lines represent dominant cleavage sites and the light dashed line represents the major, less efficient cleavage site. (c) P159 with heparin-binding domain motifs boxed and color-coded and structural features, as indicated in the key.

hyopneumoniae proteins that bound heparin agarose identified tryptic peptides of P159 spanning amino acids 47−208 and 128−198 in gel slices from 20 to 25 kDa (Fragment 27) and 15−20 kDa (Fragment 28), respectively (Figure 5).

P27 has a p*I* of ∼9.0 (Figure 2). However, anti-F1$_{P159}$ and anti-F2$_{P159}$ sera (Fragment 11) both recognized protein spots, which contain portions of P27 of 35 kDa with p*I* of 5.2−5.5. To accommodate the large shift in p*I*, we propose that Fragment 11 spans amino acids 42−361 containing acidic domain 1, generating a protein with a theoretical mass and p*I* of 35.4 kDa and 6.0 respectively. A tryptic peptide carrying a biotinylated N-terminus with the sequence ^{362}AASGLQGLLPNEYTLLPV-SSDK^{383} (Figure S2c in the Supporting Information) within P110 was detected supporting this hypothesis.

Anti-F2$_{P159}$ and anti-F3$_{P159}$ sera detected many fragments of P159. Proteins marked as P110 generated tryptic peptides (data not shown) spanning amino acids 234−981 and have a predicted p*I* of 6.16 (Figure 3) and, as expected, are recognized by anti-F2$_{P159}$ and anti-F3$_{P159}$ sera (Figure 3c,e). A 100 kDa fragment (Fragment 1) generated tryptic peptides that mapped to all but the C-terminal 10 kDa of P110 (Figure 4a). Fragment 1 has a predicted p*I* of 6.4 consistent with where it resides in Figure 3. LC−MS/MS analysis of fragments 2, 3, 4, 5, and 6 identified tryptic peptides spanning different regions of P110 that have progressively lost part of the C-terminus, react with

dx.doi.org/10.1021/pr400903s | *J. Proteome Res.* 2013, 12, 5891−5903

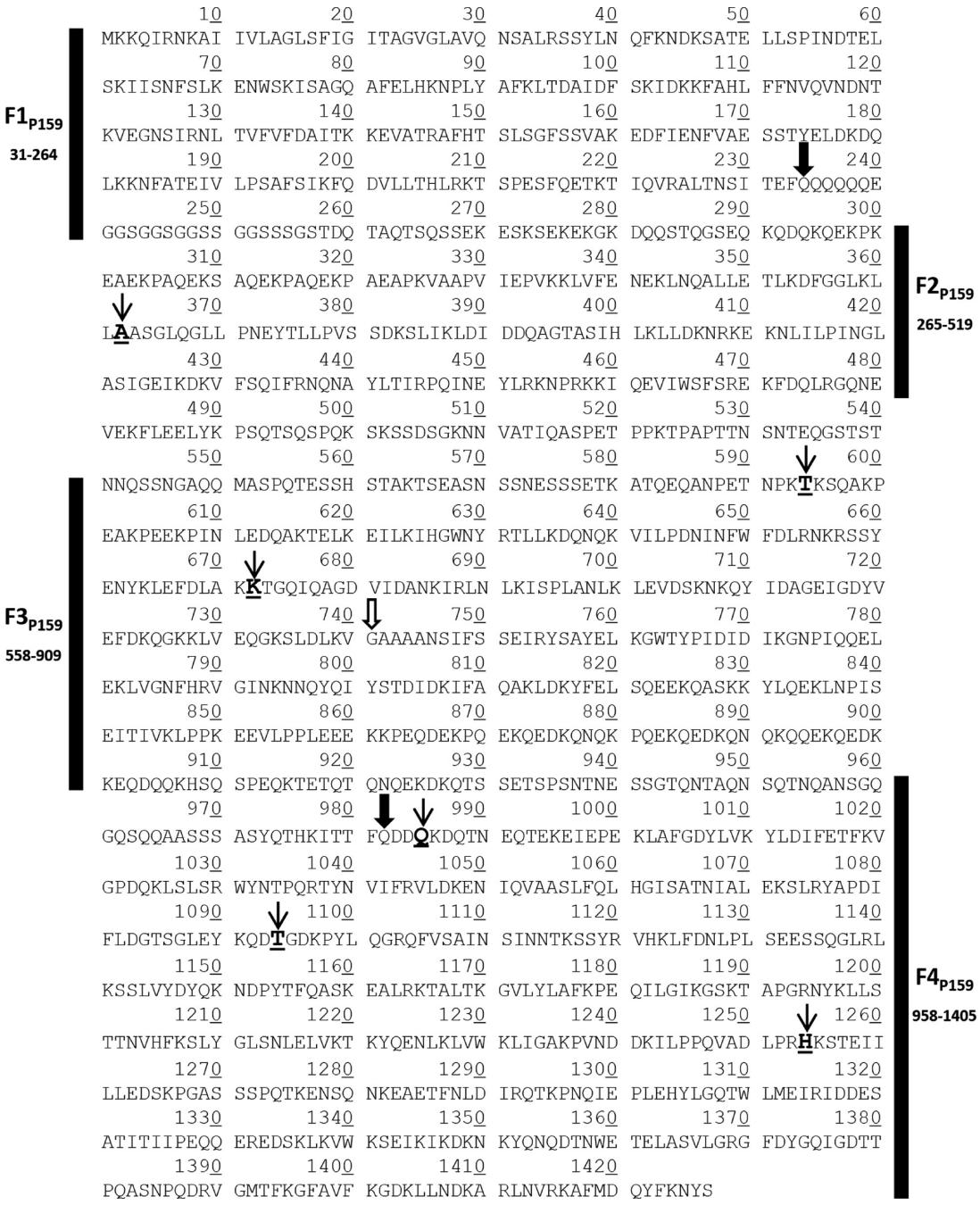

Figure 6. Dominant, major, and minor cleavage sites within P159. Solid black arrows indicate major cleavage sites that produce P27, P110, and P52, the most readily identifiable cleavage fragments of P159. The major cleavage site generating P76 and P35 is shown by a hollow arrow. The first (biotinylated) amino acid of biotinylated N-terminal peptides is shown with narrow arrows in enlarged, bold, and underlined text.

anti-$F2_{P159}$ and anti-$F3_{P159}$ sera, and display a basic p*I* (Figure 4b–f). Two peptides, ^{594}TKSQAKPEAK^{603} and ^{672}KTGQIQAGDVIDANK^{686} carrying biotinylated N-termini (Figure S2d,e in the Supporting Information) reside within P76 (Figure 6). Fragment 3 generated tryptic fragments spanning amino acids 234–740, migrated with a p*I* of 7.5 to 8.5, and reacted with anti-$F2_{P159}$ and anti-$F3_{P159}$ sera, consistent with it representing P76. Fragment 10 has an almost identical mass and p*I* to Fragment 8 (Figure 4g), but we identified the tryptic peptide ^{740}VGAAAASNIFSSEIR^{754} instead of the semitryptic peptide ^{741}GAAAANSIFSSEIR^{754}. This suggests that Fragment 10 is a slightly larger minor variant of Fragment 8, which cannot be distinguished from one another on 2D immunoblots.

Fragments 8, 9, 15, 16, and 17 are recognized by anti-$F3_{P159}$ and anti-$F4_{P159}$ on 2D immunoblots. We hypothesize that fragment 10 spans amino acids 672–1093, generating a protein with a predicted mass and p*I* of 48.2 kDa and 5.17, respectively. This fragment is generated by two cleavage events at K↓K^{672} (^{672}KTGQIQAGDVIDANK^{686}) and K↓T^{1094} (^{1094}TGDKPYLQGR^{1103}). Fragment 9 has a mass of 70 kDa and p*I* of 5.7 and was identified by LC–MS/MS analysis of protein spots cut from 2D gels (Figure 2). Fragment 9 is likely to span amino acids 594–1170, and such a fragment would display a predicted mass of 66.2 kDa and p*I* of 5.95.

Fragment 15 spans amino acids 594–1427 generating a protein with a mass of 95.6 kDa and a p*I* of 6.80. Fragment 16

dx.doi.org/10.1021/pr400903s | *J. Proteome Res.* 2013, 12, 5891–5903

has a mass of 43.6 kDa and a p*I* of 5.71. A protein that spans amino acids 672−1093 would display a mass of 48 kDa and a p*I* of 5.2. Fragment 17 has a mass of 40 kDa and a p*I* of 5.2. We predict that Fragment 17 spans amino acids 741−1093 generating a protein with a mass of 40.6 kDa and a p*I* of 5.05.

There appeared to be three cleavage fragments (Fragments 19−21) residing within P52 (Figure 3g). We identified two N-terminal biotinylated peptides within P52 (Figure S2a,b in the Supporting Information). These cleavage sites are capable of generating numerous combinations of cleavage fragments consistent with Fragments 19−21 shown in Figure 3g. These data suggest that other, as of yet uncharacterized, cleavage sites reside within P52.

Biotinylated *M. hyopneumoniae* proteins recovered by avidin chromatography were also resolved using 1D SDS-PAGE and characterized by LC−MS/MS analysis. Using this approach we identified Fragment 0 with a mass of ∼160 kDa that is recognized with anti-$F2_{P159}$, anti-$F3_{P159}$ and anti-$F4_{P159}$ sera (Figure 3d,f,h). Tryptic peptides identified by LC−MS/MS spanned P110 and P52 (amino acids 234−1427, data not shown), generating a protein with a predicted mass of 135 kDa and a p*I* of 6.98.

Identification of Regions of P159 That Bind to PK-15 Cell-Surface Proteins

We applied a systems wide strategy to identify *M. hyopneumoniae* proteins that interact with proteins that are displayed on the cell surface of porcine kidney epithelial-like cell monolayers (PK-15 cells). This approach recovered P27, P110, and P52 (data not shown) indicating that these three dominant cleavage fragments retain the ability to bind to porcine epithelial-like cells.

Regions of P159 That Bind Heparin

Heparin-binding P159 proteins displayed masses from 73 to 92 kDa (band 1, Fragment 22), 60−72 kDa (band 2, Fragment 23), 48−59 kDa (band 3, Fragment 24), 38−47 kDa (band 4, Fragment 25), 32−37 kDa (band 5, Fragment 26), 20−26 kDa (band 6, Fragment 27), and 15−19 kDa (band 7, Fragment 28) (Figure 5). Tryptic peptides generated by digesting *M. hyopneumoniae* proteins that are retained during heparin-agarose chromatography span most regions of P159, including the dominant cleavage fragments P27, P110, and P52 at their correct masses when resolved by SDS-PAGE. Consistent with these observations, the P159 protein sequence carries a wide array of putative heparin-binding motifs that span the entire molecule (Figure 5).

Regions of P159 That Bind to Porcine Cilia

We tested the ability of recombinant fragments $F1_{P159}$−$F4_{P159}$ to bind to porcine cilia using an established cilium-binding assay.[16] We show that $F2_{P159}$ and $F4_{P159}$ retain the capacity to bind cilia. $F1_{P159}$ and $F3_{P159}$ do not bind cilia (Figure 7).

DISCUSSION

P159 is one of the most highly expressed proteins in the *M. hyopneumoniae* proteome. We show that it is a target of multiple processing events that generate an extensive repertoire of fragments on the cell surface. Previously we described three cell-surface cleavage products comprising N-terminal 27 kDa, central 110 kDa, and C-terminal 52 kDa fragments, but we were unable to define the precise cleavage sites that produced them. LC−MS/MS analyses of tryptic peptides of fragments of P159 resolved by 2D SDS-PAGE identified the peptides

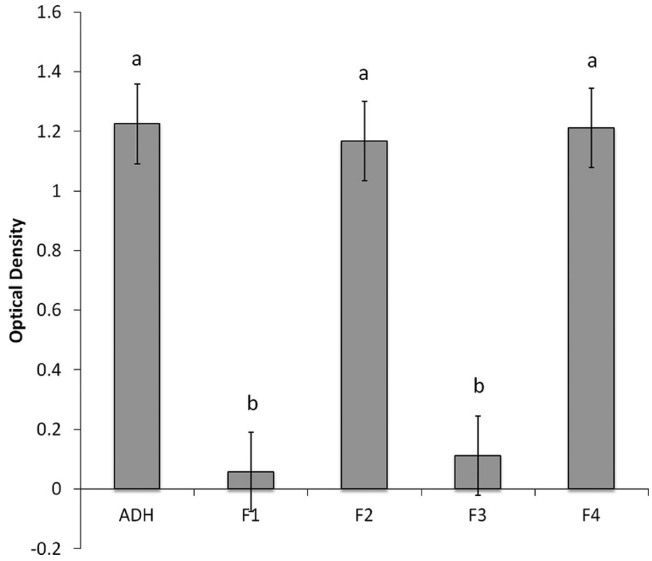

Figure 7. Binding of P159 fragments to porcine cilia. Data represent the mean ± standard error of two independent experiments, as determined by a one-way ANOVA. Data with the same labels are the same statistically ($p < 0.0001$). ADH is a positive control and represents the C-terminal fragment of P97 that contains the cilium-binding domain.[10]

^{234}QQQQQQEGG/24/SSEK^{270} and ^{982}QDDQKDQTNEQT-EK^{995} confirming that cleavage occurred at the C-terminal side of the phenylalanine residue in the motifs ^{230}I-T-E-F↓Q-Q-Q^{237} and ^{978}I-T-T-F↓Q-D-D^{984}. The ^{230}I-T-E-F↓Q-Q-Q^{237} cleavage site defines P27 as a protein that commences at position 1 and ends at position 234. The ^{978}I-T-T-F↓Q-D-D^{984} cleavage site shows that P110 spans amino acids 235−981 and P52 spans amino acids 982−1427. These cleavage sites are consistent with our previous study where we broadly mapped P27, P110, and P52 by MALDI TOF-MS.[18]

P159 is a modular protein. Domains residing within P27, P110, and P52 are flanked by large regions of protein disorder spanning more than 200 amino acids. S/T-X-F↓X-D/E cleavage sites reside within disordered regions, which are enriched in glutamine and aspartic acid residues. The disproportionate concentration of D/E residues imparts an acidic p*I* to cleavage fragments that span these domains. In contrast, regions of P159 lying outside these expansive disordered regions are enriched in K and R residues that impart a basic p*I* to endoproteolytic fragments. As a result, endoproteolytic fragments display isoelectric points ranging from 5 to 10. We were able to provide robust data to characterize a subset of 28 proteins from a much larger pool of cleavage fragments that were produced at concentrations too low for LC−MS/MS but were detectable by immunoblotting with anti-$F1_{P159}$-$F4_{P159}$ sera or enrichment protocols including avidin chromatography of biotinylated surface proteins and heparin-agarose chromatography. This remarkable observation indicates that endoproteolytic processing creates considerable surface protein diversity. Figure 8 provides a summary of cleavage fragments we found in P159.

A single heparin-binding consensus motif XBBXBX (where B represents a basic residue and X is any amino acid)[33] is located between amino acids 407−412 of P159 sequence. However, numerous putative heparin-binding motifs, including XBBXXB-XBX (452−460), XBBXXXXBX (1−9, 139−147), XBXXBX-XBXBXBX (269−281), XBXXXBXXBX (1115−1124), XBX-XXBXXBXBX (290−301, 401−412), XBXXXXBXXXXBXXXX

dx.doi.org/10.1021/pr400903s | *J. Proteome Res.* 2013, 12, 5891−5903

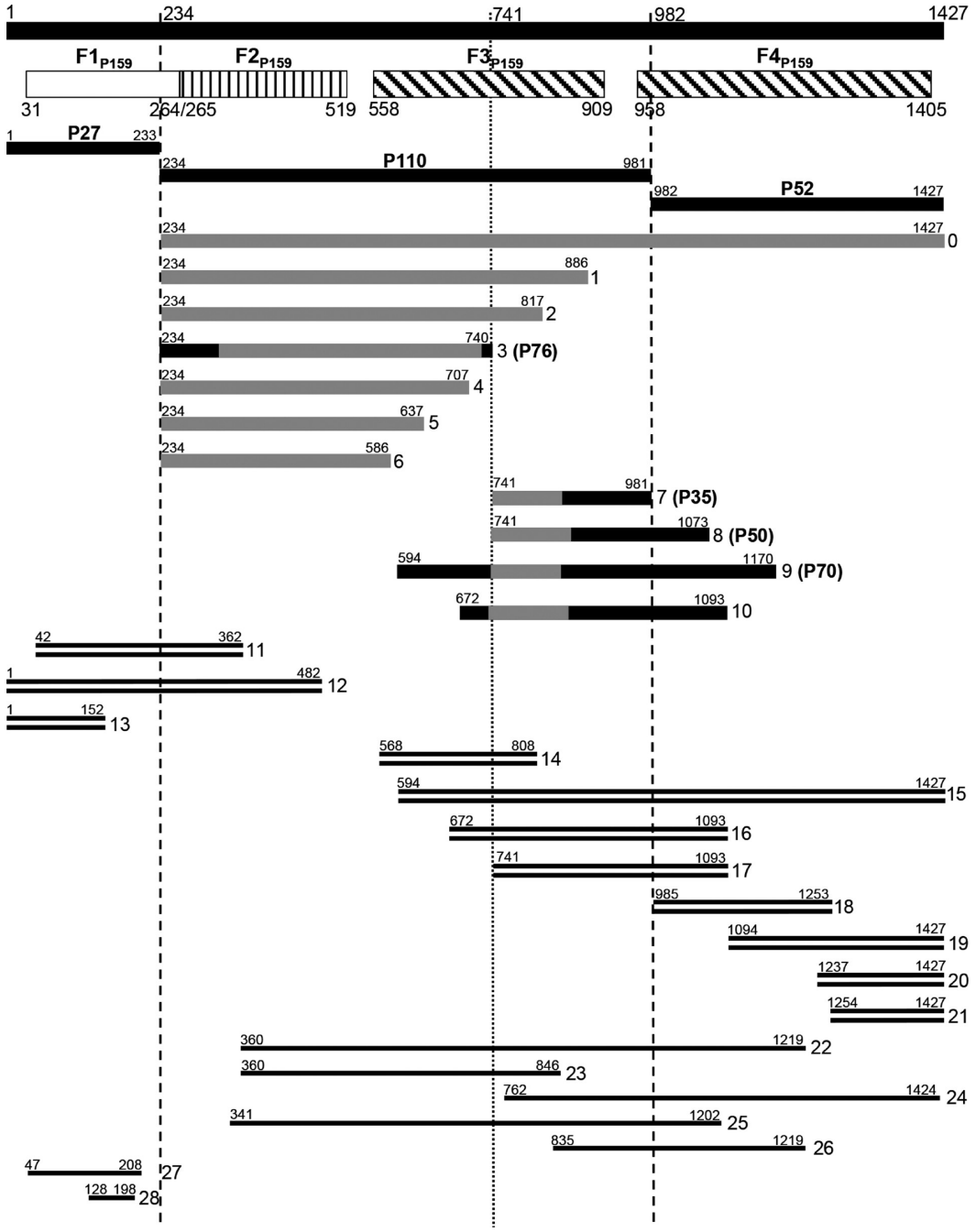

Figure 8. Schematic representation of cleavage fragments. Full-length P159 is represented by a solid black line, marked with amino acid numbers. Proteolytic cleavage sites occurring at ^{233}F↓Q^{234} and ^{981}F↓Q^{982} motif are shown by dashed vertical lines, and the cleavage site occurring at ^{738}L-K-V↓G-A-A^{743} is shown by a dotted vertical line. Recombinant proteins (F1−F4$_{P159}$) generated by Burnett et al.[18] are shown below the molecule corresponding to their positions within the molecule. Vertical and diagonal lined boxes represent fragments that were previously shown by Burnett et al. to bind PK-15 cells (F2−F4$_{P159}$), and diagonally lined boxes represent those that have been shown to bind heparin (F3$_{P159}$ and F4$_{P159}$). The dominant cleavage fragments P27, P110, and P52 reported by Burnett et al.[18] are shown below as solid black lines. Below this are less dominant cleavage fragments (gray bars) identified from single spots on 2D SDS-PAGE by LC−MS/MS. Black regions within these molecules correspond to areas with no peptide coverage but are assumed to be part of these fragments based on their observed molecular weight and p*I*. Double-lined bars represent cleavage fragments, which were identified on 2D SDS-PAGE immunoblots probed with anti-F1-F4$_{P159}$ sera. Fragments identified by heparin-pulldowns are indicated by thin black bars. (See also Figure 5.) Terminal amino acid positions are indicated above each fragment.

(303−323, 824−839, 1159−1174), XBXXXBXXXBXXX (594−608, 615−625, 867−901), and XBXBXXBXXXBXBXBXBX (1335−1350), are distributed across the P159 protein sequence and are likely to contribute to the ability of cleavage fragments to interact with mucins and epithelial cell and cilial receptors. The widespread distribution of putative heparin-binding motifs ensures that cleaved ectodomains retain an ability to bind to glycosaminoglycans that decorate the surface of porcine cilia and microvilli.[34]

We also mapped the precise cleavage event in P110 that generates P76 and P35 within the sequence ^{738}L-K-V↓G-A-A^{743} by identifying the semitryptic fragment ^{741}GAAAANSIFSSE-

dx.doi.org/10.1021/pr400903s | J. Proteome Res. 2013, 12, 5891−5903

IR[754] by LC−MS/MS. Unlike S/T-X-F↓X-D/E sites, this cleavage site does not reside within a disordered region of P159. We previously identified a cleavage site in Mhp385, a heparin-binding paralog of P97 that showed sequence similarity with [738]L-K-V↓G-A-A[743]. This cleavage event occurred at the sequence L-N-V↓A-V-S, and like [738]L-K-V↓G-A-A[743], it did not reside within a region of protein disorder. The peptide [359]K-L-L↓A-A-S[364] retains similar amino acids in key positions in the motif L-X-V↓X-V/A-X. Cleavage sites L-N-V↓A-V-S from Mhp385, [359]K-L-L↓A-A-S[364], and [738]L-K-V↓G-A-A[743] from this study all conform to a motif L-X-V↓X-V/A-X, suggesting that cleavage at these sites is performed by a protease that is different from the one that recognizes S/T-X-F↓X-D/E sites. Six N-terminal tryptic peptides that were biotinylated on their N-termini were identified by LC−MS/MS, confirming that numerous, less-abundant cleavage events occur within P159. Many P159 cleavage fragments are retained on heparin-agarose columns and span regions that bind to porcine cilia, indicating that processing releases functionally active fragments in a manner akin to ectodomain shedding in eukaryote cells.[35]

Unlike the S/T-X-F↓X-D/E cleavage motif, we were not able to decipher the sequence of motifs that produced low abundance cleavage fragments. Nonetheless, three of the six N-terminal fragments were bona-fide tryptic peptides, suggesting that a trypsin-like protease may be functionally active on the surface of *M. hyopneumoniae*. Our data suggest that once the major cleavage fragments have been generated, they become susceptible to further proteolytic cleavage. Alternatively, the N-termini of the major cleavage fragments may be targeted by aminopeptidases that recover amino acids essential for growth. Recently, we showed that MHJ_0125 is a multifunctional protein that displays glutamyl-aminopeptidase activity and moonlights as a plasminogen-binding protein on the cell surface of *M. hyopneumoniae*.[21] However, we have not shown that the MHJ_0125 targets *M. hyopneumoniae* proteins. In the current study, the peptide [985]QKDQTNEQTEKEIEPEK[1001] was identified as a biotinylated N-terminal peptide (Figure S3 in the Supporting Information). This peptide sequence commences three amino acids downstream of the N-terminal fragment [982]↓QDDQKDQTNEQTEK[995] that separates P52 from P110. The [985]QKDQTNEQTEKEIEPEK[1001] peptide is unusual because it is semitryptic and may be the product of aminopeptidase activity.

P159 encodes a single transmembrane domain spanning amino acids 9−29 (TmPred score 2050). We previously showed that transmembrane domains found in members of the P97 and P102 paralog families are not removed during secretion to the cell surface. Consequently, P27 and larger low-abundance N-terminal fragments that include parts of P110 are expected to remain embedded in the *M. hyopneumoniae* cell membrane. Many P159 fragments do not carry a transmembrane sequence. It is remarkable that we were able to detect evidence of most cleavage fragments as many are expected to be shed into the extracellular milieu where conceivably they (i) bind target cell receptors, (ii) act as decoys for effector molecules of the porcine immune response, and (iii) represent docking sites that promote homopolymeric interactions for cell−cell contact and biofilm formation. The high serum content found in *M. hyopneumoniae* medium precludes studies that seek to detect shed cleavage fragments. Several host molecules including fibronectin and plasminogen are known to be sequestered onto the surface of *M. hyopneumoniae*, and these may provide a scaffold for retaining cleavage fragments.[9−11,13−15,17,21]

Surface-accessible membrane proteins in eukaryotes are known to be released into the extracellular milieu via a process known as ectodomain shedding.[35] Ectodomain shedding is now recognized as a widespread process in eukaryotes, and algorithms have been developed to identify membrane proteins that are targeted by sheddases.[36] Previous studies in eukaryote systems suggested that ∼4% of surface associated proteins are targets for ectodomain shedding.[37] Shed proteins regulate neuron migration, osteoclast development, the differentiation and proliferation of hematopoietic precursor cells, cell fate, and the presentation of CD44[38−40] underscoring the biological utility of this process. These data are consistent with the notion that many, if not all, proteins are multifunctional and highlight that the informational content of proteins is likely to be significantly underestimated.

The S/T-X-F↓X-D/E motif is now firmly established as a site where dominant cleavage occurs in major adhesin families of *M. hyopneumoniae*. Our initial surfaceome studies show that ∼150 ORFs can be detected on the surface of *M. hyopneumoniae* using biotinylation and trypsin-shaving strategies (data not shown). Our studies with members of the P97 and P102 paralog families[9−18] and P159 presented here indicate that cleavage may be a complex, sophisticated mechanism to generate surface protein diversity in a manner akin to ectodomain shedding. We are now determining how many proteins on the surface of *M. hyopneumoniae* are targets of endoproteolytic activity. Previously, we provided evidence that abundantly expressed surface proteins in Gram negative gastrointestinal pathogen *Campylobacter jejuni*,[41] Gram positive pathogen *Streptococcus pyogenes*,[42] and the avian pathogen *Mycoplasma gallisepticum*[25] are presented on the cell surface as protein fragments, indicating that they are targets of endoproteolytic processing. Further studies are needed to examine the role of endoproteolysis of surface proteins in pathogenesis and prokaryote biology more broadly.

■ CONCLUSIONS

P159 (MHJ_0494) is a highly expressed, extensively processed, surface-accessible molecule that shares functional similarities with members of the P97 and P102 paralog families. Cleavage fragments of P159 display a remarkable capacity to bind to glycosaminoglycans and function as epithelial cell[18] and cilium adhesins. It is now clear that proteolytic processing represents the principal means by which *M. hyopneumoniae* generates surface protein diversity and functional redundancy in glycosaminoglycan- and cilium-binding.[9−19,21] Processing events presumably have evolved to ensure that *M. hyopneumoniae* is adept at colonizing and persisting within the porcine respiratory tract and potentially at other organ sites in the face of an immunological assault from the host. Endoproteolysis of adhesin families in the genome-reduced microbial pathogen *M. hyopneumoniae* displays all hallmarks of ectodomain shedding, a process that has evolved to generate functional diversity in eukaryotes.

■ ASSOCIATED CONTENT

Supporting Information

Spectra supporting the identification of biotinylated and semitryptic peptides. This material is available free of charge via the Internet at http://pubs.acs.org.

AUTHOR INFORMATION

Corresponding Author

*E-mail: Steven.Djordjevic@uts.edu.au. Phone: +612 9514 4127. Fax: +612 9514 4143.

Author Contributions

§B.B.A.R. and J.L.T. contributed equally to this work.

Notes

The authors declare no competing financial interest.

ACKNOWLEDGMENTS

B.B.A.R and J.L.T are recipients of Doctoral Scholarships from University of Technology, Sydney. V.M.J. is the recipient of an Australian Postgraduate Award.

REFERENCES

(1) Haesebrouck, F.; Pasmans, F.; Chiers, K.; Maes, D.; Ducatelle, R.; Decostere, A. Efficacy of vaccines against bacterial diseases in swine: what can we expect? *Vet. Microbiol.* **2004**, *100* (3−4), 255−268.

(2) Maes, D.; Segales, J.; Meyns, T.; Sibila, M.; Pieters, M.; Haesebrouck, F. Control of *Mycoplasma hyopneumoniae* infections in pigs. *Vet. Microbiol.* **2008**, *126* (4), 297−309.

(3) Thacker, E. L. Mycoplasmal Diseases. In *Diseases of Swine*, 9th ed.; Straw, B, Ed.; Blackwell Publishing: Ames, IA, 2006.

(4) Thacker, E. L.; Halbur, P. G.; Ross, R. F.; Thanawongnuwech, R.; Thacker, B. J. *Mycoplasma hyopneumoniae* potentiation of porcine reproductive and respiratory syndrome virus-induced pneumonia. *J. Clin. Microbiol.* **1999**, *37* (3), 620−627.

(5) Thacker, E. L.; Thacker, B. J.; Young, T. F.; Halbur, P. G. Effect of vaccination on the potentiation of porcine reproductive and respiratory syndrome virus (PRRSV)-induced pneumonia by *Mycoplasma hyopneumoniae*. *Vaccine* **2000**, *18* (13), 1244−52.

(6) Minion, C. F.; Lefkowitz, E. J.; Madsen, M. L.; Cleary, B. J.; Swartzell, S. M.; Mahairas, G. G. The Genome Sequence of *Mycoplasma hyopneumoniae* Strain 232, the Agent of Swine Mycoplasmosis. *J. Bacteriol.* **2004**, *186* (21), 11.

(7) Kobisch, M.; Blanchard, B.; Le Potier, M. F. *Mycoplasma hyopneumoniae* infection in pigs: duration of the disease and resistance to reinfection. *Vet. Res.* **1993**, *24* (1), 67−77.

(8) Mebus, C. A.; Underdahl, N. R. Scanning electron microscopy of trachea and bronchi from gnotobiotic pigs inoculated with *Mycoplasma hyopneumoniae*. *Am. J. Vet. Res.* **1977**, *38* (8), 1249−54.

(9) Bogema, D. R.; Scott, N. E.; Padula, M.; Tacchi, J. L.; Raymond, B. B.; Jenkins, C.; Cordwell, S. J.; Minion, F. C.; Walker, M. J.; Djordjevic, S. P. The sequence TTKF↓QE defines the site of proteolytic cleavage in Mhp683, a novel glycosaminoglycan and cilium adhesin of *Mycoplasma hyopneumoniae*. *J. Biol. Chem.* **2011**, *286*, 41217−41229.

(10) Deutscher, A. T.; Jenkins, C.; Minion, F. C.; Seymour, L. M.; Padula, M. P.; Dixon, N. E.; Walker, M. J.; Djordjevic, S. P. Repeat regions R1 and R2 in the P97 paralogue Mhp271 of *Mycoplasma hyopneumoniae* bind heparin, fibronectin and porcine cilia. *Mol. Microbiol.* **2010**, *78* (2), 444−58.

(11) Deutscher, A. T.; Tacchi, J. L.; Minion, F. C.; Padula, M. P.; Crossett, B.; Bogema, D. R.; Jenkins, C.; Kuit, T. A.; Walker, M. J.; Djordjevic, S. P. *Mycoplasma hyopneumoniae* Surface Proteins Mhp385 and Mhp384 Bind Host Cilia and Glycosaminoglycans and Are Endoproteolytically Processed by Proteases That Recognize Different Cleavage Motifs. *J. Proteome Res.* **2012**, *11*, 1924−1936.

(12) Djordjevic, S. P.; Cordwell, S. J.; Djordjevic, M. A.; Wilton, J.; Minion, F. C. Proteolytic processing of the *Mycoplasma hyopneumoniae* cilium adhesin. *Infect. Immun.* **2004**, *72* (5), 2791−2802.

(13) Seymour, L. M.; Deutscher, A. T.; Jenkins, C.; Kuit, T. A.; Falconer, L.; Minion, F. C.; Crossett, B.; Padula, M.; Dixon, N. E.; Djordjevic, S. P.; Walker, M. J. A processed multidomain *Mycoplasma hyopneumoniae* adhesin binds fibronectin, plasminogen, and swine respiratory cilia. *J. Biol. Chem.* **2010**, *285* (44), 33971−8.

(14) Seymour, L. M.; Falconer, L.; Deutscher, A. T.; Minion, F. C.; Padula, M. P.; Dixon, N. E.; Djordjevic, S. P.; Walker, M. J. Mhp107 is a member of the multifunctional adhesin family of *Mycoplasma hyopneumoniae*. *J. Biol. Chem.* **2011**, *286* (12), 10097−104.

(15) Seymour, L. M.; Jenkins, C.; Deutscher, A. T.; Raymond, B. B.; Padula, M. P.; Tacchi, J. L.; Bogema, D. R.; Eamens, G. J.; Woolley, L. K.; Dixon, N. E.; Walker, M. J.; Djordjevic, S. P. Mhp182 (P102) binds fibronectin and contributes to the recruitment of plasmin(ogen) to the *Mycoplasma hyopneumoniae* cell surface. *Cell Microbiol.* **2012**, *14* (1), 81−94.

(16) Wilton, J.; Jenkins, C.; Cordwell, S. J.; Falconer, L.; Minion, F. C.; Oneal, D. C.; Djordjevic, M. A.; Connolly, A.; Barchia, I.; Walker, M. J.; Djordjevic, S. P. Mhp493 (P216) is a proteolytically processed, cilium and heparin binding protein of *Mycoplasma hyopneumoniae*. *Mol. Microbiol.* **2009**, *71* (3), 566−582.

(17) Bogema, D. R.; Deutscher, A. T.; Woolley, L. K.; Seymour, L. M.; Raymond, B. B.; Tacchi, J. L.; Padula, M. P.; Dixon, N. E.; Minion, F. C.; Jenkins, C.; Walker, M. J.; Djordjevic, S. P. Characterization of cleavage events in the multifunctional cilium adhesin Mhp684 (P146) reveals a mechanism by which *Mycoplasma hyopneumoniae* regulates surface topography. *mBio* **2012**, *3* (2), e00282-11.

(18) Burnett, T. A.; Dinkla, K.; Rohde, M.; Chhatwal, G. S.; Uphoff, C.; Srivastava, M.; Cordwell, S. J.; Geary, S.; Liao, X.; Minion, C. F.; Walker, M. J.; Djordjevic, S. P. P159 is a proteolytically processed, surface adhesin of *Mycoplasma hyopneumoniae*: Defined domains of P159 bind heparin and promote adherence to eukaryote cells. *Mol. Microbiol.* **2006**, *60* (3), 18.

(19) Jenkins, C.; Wilton, J. L.; Minion, F. C.; Falconer, L.; Walker, M. J.; Djordjevic, S. P. Two domains within the *Mycoplasma hyopneumoniae* cilium adhesin bind heparin. *Infect. Immun.* **2006**, *74* (1), 481−487.

(20) Zhang, Q.; Young, T. F.; Ross, R. F. Microtiter plate adherence assay and receptor analogs for *Mycoplasma hyopneumoniae*. *Infect. Immun.* **1994**, *62* (5), 1616−22.

(21) Robinson, M. W.; Buchtmann, K. A.; Jenkins, C.; Tacchi, J. L.; Raymond, B. B.; To, J.; Roy Chowdhury, P.; Woolley, L. K.; Labbate, M.; Turnbull, L.; Whitchurch, C. B.; Padula, M. P.; Djordjevic, S. P. MHJ_0125 is an M42 glutamyl aminopeptidase that moonlights as a multifunctional adhesin on the surface of *Mycoplasma hyopneumoniae*. *Open Biol.* **2013**, *3* (4), 130017.

(22) Friis, N. F. Some recommendations concerning primary isolation of *Mycoplasma suipneumoniae* and *Mycoplasma flocculare* a survey. *Nord Veterinaermed.* **1975**, *27* (6), 337−9.

(23) Scarman, A. L.; Chin, J. C.; Eamens, G. J.; Delaney, S. F.; Djordjevic, S. P. Identification of novel species-specific antigens of *Mycoplasma hyopneumoniae* by preparative SDS-PAGE ELISA profiling. *Microbiology* **1997**, *143* (Pt 2), 663−73.

(24) Nunomura, K.; Nagano, K.; Itagaki, C.; Taoka, M.; Okamura, N.; Yamauchi, Y.; Sugano, S.; Takahashi, N.; Izumi, T.; Isobe, T. Cell surface labeling and mass spectrometry reveal diversity of cell surface markers and signaling molecules expressed in undifferentiated mouse embryonic stem cells. *Mol. Cell. Proteomics* **2005**, *4* (12), 1968−76.

(25) Szczepanek, S. M.; Frasca, S., Jr.; Schumacher, V. L.; Liao, X.; Padula, M.; Djordjevic, S. P.; Geary, S. J. Identification of lipoprotein MslA as a neoteric virulence factor of *Mycoplasma gallisepticum*. *Infect. Immun.* **2010**, *78* (8), 3475−83.

(26) Kyhse-Andersen, J. Electroblotting of multiple gels: a simple apparatus without buffer tank for rapid transfer of proteins from polyacrylamide to nitrocellulose. *J. Biochem. Biophys. Methods* **1984**, *10* (3−4), 203−9.

(27) Chen, B.; Zhang, A.; Xu, Z.; Li, R.; Chen, H.; Jin, M. Large-scale identification of bacteria-host crosstalk by affinity chromatography: capturing the interactions of *Streptococcus suis* proteins with host cells. *J. Proteome Res.* **2011**, *10* (11), 5163−74.

(28) Wilkins, M. R.; Gasteiger, E.; Bairoch, A.; Sanchez, J. C.; Williams, K. L.; Appel, R. D.; Hochstrasser, D. F. Protein identification and analysis tools in the ExPASy server. *Methods Mol. Biol.* **1999**, *112*, 531−52.

(29) Lupas, A.; Van Dyke, M.; Stock, J. Predicting coiled coils from protein sequences. *Science* **1991**, *252* (5009), 1162−4.
(30) Obradovic, Z.; Peng, K.; Vucetic, S.; Radivojac, P.; Dunker, A. K. Exploiting heterogeneous sequence properties improves prediction of protein disorder. *Proteins* **2005**, *61* (Suppl 7), 176−82.
(31) Su, H. C.; Hutchison, C. A., 3rd; Giddings, M. C. Mapping phosphoproteins in Mycoplasma genitalium and Mycoplasma pneumoniae. *BMC Microbiol.* **2007**, *7*, 63.
(32) Righetti, P. G. Real and imaginary artefacts in proteome analysis via two-dimensional maps. *J. Chromatogr., B* **2006**, *841* (1−2), 14−22.
(33) Cardin, A. D.; Weintraub, H. J. Molecular modeling of protein-glycosaminoglycan interactions. *Arteriosclerosis* **1989**, *9* (1), 21−32.
(34) Erlinger, R. Glycosaminoglycans in porcine lung: an ultra-structural study using cupromeronic blue. *Cell Tissue Res.* **1995**, *281* (3), 473−83.
(35) Horiuchi, K. A brief history of tumor necrosis factor alpha–converting enzyme: an overview of ectodomain shedding. *Keio J. Med.* **2013**, *62* (1), 29−36.
(36) Tien, W. S.; Chen, Y. T.; Wu, K. P. SecretePipe: a screening pipeline for secreted proteins with competence to identify potential membrane-bound shed markers. *J. Proteome Res.* **2013**, *12* (3), 1235−44.
(37) Arribas, J.; Massague, J. Transforming growth factor-alpha and beta-amyloid precursor protein share a secretory mechanism. *J. Cell Biol.* **1995**, *128* (3), 433−41.
(38) Yamagishi, S.; Hampel, F.; Hata, K.; Del Toro, D.; Schwark, M.; Kvachnina, E.; Bastmeyer, M.; Yamashita, T.; Tarabykin, V.; Klein, R.; Egea, J. FLRT2 and FLRT3 act as repulsive guidance cues for Unc5-positive neurons. *EMBO J.* **2011**, *30* (14), 2920−33.
(39) Sanderson, M. P.; Abbott, C. A.; Tada, H.; Seno, M.; Dempsey, P. J.; Dunbar, A. J. Hydrogen peroxide and endothelin-1 are novel activators of betacellulin ectodomain shedding. *J. Cell Biochem.* **2006**, *99* (2), 609−23.
(40) Stoeck, A.; Keller, S.; Riedle, S.; Sanderson, M. P.; Runz, S.; Le Naour, F.; Gutwein, P.; Ludwig, A.; Rubinstein, E.; Altevogt, P. A role for exosomes in the constitutive and stimulus-induced ectodomain cleavage of L1 and CD44. *Biochem. J.* **2006**, *393* (Pt 3), 609−18.
(41) Scott, N. E.; Marzook, N. B.; Deutscher, A.; Falconer, L.; Crossett, B.; Djordjevic, S. P.; Cordwell, S. J. Mass spectrometric characterization of the *Campylobacter jejuni* adherence factor CadF reveals post-translational processing that removes immunogenicity while retaining fibronectin binding. *Proteomics* **2010**, *10* (2), 277−88.
(42) Cole, J. N.; Ramirez, R. D.; Currie, B. J.; Cordwell, S. J.; Djordjevic, S. P.; Walker, M. J. Surface analyses and immune reactivities of major cell wall-associated proteins of group a streptococcus. *Infect. Immun.* **2005**, *73* (5), 3137−46.